frontiers in Environmental Science

ORIGINAL RESEARCH
published: 24 February 2022
doi: 10.3389/fenvs.2022.815528

Calcium-Mediated Regulation Promotes the Biofilm Formation of Two Novel Pyridine-Degrading Bacteria

Fuzhong Xiong[1], *Donghui Wen*[1]* *and Qilin Li*[2]

[1]College of Environmental Sciences and Engineering, Peking University, Beijing, China, [2]Department of Civil and Environmental Engineering, Rice University, Houston, TX, United States

In bioaugmented wastewater treatment systems, it is essential for recalcitrant pollutant-degrading bacteria to form biofilms. Inducing biofilm formation in these bacteria, however, is challenging as it involves multiple inter-related regulating pathways and environmental factors. Herein, we report the remarkable promoting effect of Ca^{2+} on biofilm formation of two novel pyridine-degrading bacteria with poor innate biofilm-forming capabilities, *Pseudomonas* sp. ZX01 and *Arthrobacter* sp. ZX07. The roles of Ca^{2+} in different biofilm development stages were investigated. Our data showed strong influences of Ca^{2+} on the initial attachment of the two strains onto positively charged glass surfaces by altering cell surface charge as well as the cation bridging effect. Contrary to many other biofilm promoting mechanisms, Ca^{2+} downregulated the extracellular polymeric substances (EPS) production per cell in both *Pseudomonas* sp. ZX01 and *Arthrobacter* sp. ZX07, while increasing biofilm biomass. This is attributed to the strong cationic bridging between Ca^{2+} and EPS which can elevate the efficiency of the extracellular products in binding bacterial cells. Furthermore, Ca^{2+} increased the protein-to-polysaccharide (PN/PS) ratio in biofilm EPS of both strains, which favored cell aggregation, and biofilm establishment by increasing the hydrophobicity of cell surfaces. More intriguingly, the intracellular c-di-GMP, which can drive the switch of bacterial lifestyle from planktonic state to biofilm state, was also elevated markedly by exogenous Ca^{2+}. Taken together, these results would be of guidance for applying the two strains into bioaugmented biofilm reactors where Ca^{2+} supplement strategy can be employed to facilitate their biofilm formation on the surfaces of engineering carriers.

Keywords: biofilm formation, calcium cation, cell-to-surface attachment, cationic bridging, extracellular polymeric substances (EPS), c-di-GMP

OPEN ACCESS

Edited by:
Zifu Li,
University of Science and Technology Beijing, China

Reviewed by:
Yichao Wu,
Huazhong Agricultural University, China
Hongbo Liu,
University of Shanghai for Science and Technology, China

***Correspondence:**
Donghui Wen
dhwen@pku.edu.cn

Specialty section:
This article was submitted to Water and Wastewater Management, a section of the journal Frontiers in Environmental Science

Received: *15 November 2021*
Accepted: *10 February 2022*
Published: *24 February 2022*

Citation:
Xiong F, Wen D and Li Q (2022) Calcium-Mediated Regulation Promotes the Biofilm Formation of Two Novel Pyridine-Degrading Bacteria. Front. Environ. Sci. 10:815528. doi: 10.3389/fenvs.2022.815528

INTRODUCTION

Nitrogenous heterocyclic compounds (NHCs) such as pyridine and quinoline are toxic organic pollutants commonly found in wastewater from coal coking, gasification, and refining processes in coal chemical industries (Bai et al., 2010; Xu et al., 2015). Due to their high polarity, once released into the environment, they can spread quickly, and exert harmful effects on ecological systems and human health (Kaiser et al., 1996; Thomsen and Kilen, 1998; Bi et al., 2006). Furthermore, their stable structures make them highly resistant to conventional biological wastewater treatment employing

common microorganisms (Liang et al., 2018). Therefore, bioaugmentation, which utilizes selected microorganisms capable of degrading these recalcitrant organic pollutants, is getting increasing attention and is regarded as an effective, and economically feasible solution (Herrero and Stuckey, 2015). For example, taken pyridine as a target pollutant, various bacteria belonging to the genus of *Micrococcus* (Sims et al., 1986), *Rhizobium* (Shen et al., 2015), *Shinella* (Bai et al., 2009), *Paracoccus* (Bai et al., 2008), and *Pseudomonas* (Mohan et al., 2003) have been isolated and used for degradation of pyridine in wastewater treatment. However, the application of the bioaugmentation strategy also faces many challenges. In particular, the inoculated bacteria often fail to colonize in the microbial community due to inhospitable conditions or intense competition from indigenous species (Raper et al., 2018). Fu et al. (2009) reported that the inoculated strain disappeared from a biological aerated filter (BAF) within 3 days and attributed it to its poor biofilm-forming ability. On the other hand, strategies that promote the formation of stable biofilms by the inoculated bacteria on carriers have been shown to improve the degradation of target pollutants in bioaugmented systems (Zhao B. et al., 2018; Yue et al., 2018). However, the existing knowledge of efficiently regulating bacterial biofilm formation is obscured especially in the field of wastewater treatment engineering.

Biofilms are well-organized microbial communities, in which cells adhere to biotic or abiotic surfaces and are covered by a self-secreted extracellular polymeric substances (EPS) matrix. They represent the most widespread lifestyle for microbes (Stoodley et al., 2002; Flemming and Wuertz, 2019). Compared to the planktonic lifestyle, biofilms provide a range of advantages for microbial cells to enhance the stability of community structures, and their resistance to unfavorable conditions or environmental shock loads by enhancing intercellular communication and cooperation (Jefferson, 2004; Flemming et al., 2016). Biofilm formation is a complex, multi-step process involving various self-regulated mechanisms, e.g., quorum sensing (QS) (da Silva et al., 2017), bis-(3′-5′)-cyclic dimeric guanosine monophosphate (c-di-GMP) signaling (Wu et al., 2015), and flagella and pili mediated motility (Van Houdt and Michiels, 2005), as well as multiple surface properties including hydrophilicity and surface charge (Renner and Weibel, 2011). Moreover, biofilm development is influenced by many environmental factors such as temperature, pH, nutrients, hydraulic shear force, osmotic pressure, and divalent cations (Rinaudi et al., 2006; Zhou et al., 2013; Gomes et al., 2014). Therefore, to promote biofilm formation of the inoculated bacteria in bioaugmented reactors, it is important to identify the most crucial ones from those intricate factors.

Calcium cation (Ca^{2+}) has been widely recognized as the important second messenger in bacterial cells, participating in modulating many cellular activities and metabolic pathways (Dominguez et al., 2015; Parker et al., 2016). Many studies noted that calcium played non-negligible roles in the formation of bacterial biofilms, yet the effects varied widely in different bacterial species. For instance, calcium was found to stimulate cell-to-cell adhesion and biofilm establishment of *Pseudomonas mendocina* NR802 (Mangwani et al., 2014), *Citrobacter werkmanii* BF-6 (Zhou et al., 2016), *Bacillus* sp. (He et al., 2016), *Flavobacterium columnare* (Cai et al., 2019), and *Vibrio fischeri* (Tischler et al., 2018); but it was also shown to inhibit biofilm formation of *Staphylococcus aureus* (Shukla and Rao, 2013), and *Vibrio cholerae* (Bilecen and Yildiz, 2009). In these previous studies, calcium was found to alter cell surface charge and the electrical double layer (Marcinakova et al., 2010), elevate the production of extracellular proteins and polysaccharides (Mangwani et al., 2014; He et al., 2016), and enhance cationic bridging between bacterial cells via its interactions with EPS components such as extracellular DNA (eDNA) (Das et al., 2014). However, the specific mechanisms through which calcium mediates bacterial adhesion and subsequent biofilm formation remain inconclusive and even a subject of controversy. Moreover, the bacteria species ever studied are mainly model species or from clinical, food-related, plant-related, and marine environments. Thus, it necessitates investigating more bacterial strains from wastewater treatment plants.

In this study, we evaluated the effects of calcium on the biofilm establishment and architecture of two pyridine-degrading bacteria, *Pseudomonas* sp. ZX01 and *Arthrobacter* sp. ZX07. The underlying mechanisms of calcium-mediated regulation were also explored from the perspectives of initial cell-to-surface attachment, EPS production, and c-di-GMP signaling. The purpose of this study was to provide a fundamental understanding of the roles that calcium plays in regulating bacterial biofilm-forming behaviors, and practical guidelines for more efficient application of the two NHC-degrading strains in bioaugmented biofilm reactors.

MATERIALS AND METHOD

Chemicals

Tryptone and yeast extract were purchased from Oxoid (United Kingdom). 1% (w/v) crystal violet solution, phosphate buffered saline (PBS), and BCA Protein Assay Kit were purchased from Solarbio (China). The fluorescent dyes, SYTO9 and tetramethyl-rhodamine conjugates of concanavalin A (conA-T), were obtained from Invitrogen (United States). All the other conventional inorganic or organic chemicals used in the study were of analytical grade.

Bacterial Strains and Medium

Pseudomonas sp. ZX01 and *Arthrobacter* sp. ZX07, isolated from the activated sludge of a coking wastewater treatment plant, were chosen as the representative research objects, for they were Gram-negative and Gram-positive, respectively. The two strains could grow by taking pyridine as the sole carbon and nitrogen source and showed highly efficient pyridine-degrading abilities. Their 16S rRNA gene sequences can be obtained in GenBank database of NCBI with accession numbers MG760359 and MG760365. The main biochemical characteristics of the two strains were also

summarized in **Supplementary Table S1**. Particularly, the motility of the two strains was tested using the method described in **Supplementary Text S1**. The Luria-Bertani (LB) medium (Sezonov et al., 2007) containing 10 g/L tryptone, 5 g/L yeast extract, and 10 g/L NaCl was used for bacteria enrichment and biofilm formation.

Biofilm Cultivation and Quantification

Microtiter plate biofilm formation assay (O'Toole, 2011) was used to culture and quantify biofilm with some modifications, for its advantages in accuracy, repeatability, and batch processing. Firstly, the bacterial strain was grown in LB medium at 37°C to middle exponential phase until OD_{600} = 1.0 and washed twice with 0.9% NaCl. Then the harvested cells were resuspended in LB medium with a final OD_{600} of 0.5. Next, 1 ml cell suspension was seeded in each well of 12-well polystyrene plates (Corning, United States) and incubated at 35°C for 24 h with a shaking speed of 150 rpm. The plates containing LB medium only were taken as the negative control. After incubation, the OD_{600} of bacterial suspension in each well was measured to represent the planktonic cell growth. Then the suspension was discarded and each well was washed three times with sterile water to remove non-adherent cells. The 12-well plates were air-dried at 60°C for 1 h and 2 ml 0.1% crystal violet solution was added into each well to stain the attached biofilm cells for 25 min. Subsequently, the excess dye was rinsed off with sterile water. After drying at 35°C for 1 h again, 4 ml 95% ethanol was added into each well to redissolve the cell-bound crystal violet. Finally, 125 µl solution from each well was transformed to 96-well plates and OD_{595} was determined using a microplate reader (BioTek Synergy, United States) to represent the biofilm biomass.

In the experiments studying the effects of Ca^{2+} on biofilm formation of the two strains, different concentrations of $CaCl_2$ (i.e., 1, 2, 4, 8, 16, 32, and 64 mM) were added into the medium. For each of the experimental conditions, the assay was performed in triplicate.

Bacterial Initial Attachment Assay

To investigate the effects of Ca^{2+} on bacterial initial attachment, the attachment of the two strains to the glass slides under different Ca^{2+} concentrations were analyzed according to Ramsey and Whiteley (2004) with modifications. Briefly, the bacterial cells in the middle exponential phase were diluted in 15 ml LB medium to a final OD_{600} of 0.5; different concentrations of $CaCl_2$ (i.e., 1, 4, 16, 32, and 64 mM) were also added into the medium. The prepared bacterial culture was then poured into a 90 × 14 mm Petri dish in which a glass slide (75 × 25 mm; Jingan, China) was placed and incubated at 35°C for 1 h with a shaking speed of 90 rpm. After incubation, the glass slide was taken out and rinsed twice with PBS to remove non-adherent cells. Then the glass slide was put into a centrifuge tube with 25 ml 0.9% NaCl and vibrated intensely with a vortex mixer for 30 min to detach the cells. The number of the bacterial cells in the solution was determined using a standard plate counting method and normalized to the area of glass slides as the initial attachment index. All the assays were performed in triplicate.

EPS Extraction and Analysis

EPS was extracted from both planktonic cells and biofilms using a heating method following Bourven et al. (2011) with certain adjustments. The bacterial strain was firstly inoculated in 12-well plates as previously described. Then the suspension in each well was collected and centrifuged. The cell pellets were resuspended in 15 ml 0.9% NaCl and heated in 85°C water bath for 35 min. After filtration with 0.22 µm filters, the filtrate was collected as EPS from planktonic cells. The 12-well plate with biofilms was rinsed gently twice with sterile water and 1 ml 0.9% NaCl was added into each well of the plate. Then the plate was heat-treated and the suspensions in each well were combined. The resulting filtrate was considered EPS from the biofilms. Moreover, planktonic cells and biofilm cells on the filter were also dried and weighed.

The polysaccharide (PS) and protein (PN) content of the EPS were determined using the phenol-sulfuric acid method (Dubois et al., 1956) and the bicinchoninic acid (BCA) protein assay (Redinbaugh and Turley, 1986), respectively. The final concentrations of PN and PS were normalized by the weight of the planktonic or biofilm cells. The experiments for each condition were conducted in triplicate and each measurement was performed at least 3 times. Furthermore, the fluorescence excitation-emission matrix (EEM) analysis of the EPS from both biofilms and planktonic cells was performed using a HORIBA Aqualog spectrofluorometer. The details of EEM analysis were described in **Supplementary Text S2**.

Biofilm Observation by Confocal Scanning Laser Microscopy

The architecture and composition of biofilms formed by the two strains under different Ca^{2+} concentrations were analyzed using CLSM combined with a double staining method (Yu et al., 2016). Briefly, 700 µl of the bacterial suspension (OD_{600} = 0.5) were inoculated in a µ-Slide chambered coverslip with four wells (ibidi, Germany) and cultured at 35°C at 90 rpm in a rotary shaker for 24 h. After incubation, the chambered coverslip was rinsed twice with PBS to remove planktonic cells. Then the cells and polysaccharides in the biofilms were stained with 10 µM SYTO9 and 200 µg/ml conA-T in the dark for 30°min, respectively. After washing with PBS, the chambered coverslip was observed by a CLSM system (Leica TCS SP8, Germany) and Z-stack two-dimensional images (scanned every 0.5 µm) were obtained from at least three random areas for each sample. The 3-D images were rebuilt using IMARIS software (V9.2.1; Bitplane, Switzerland) and analyzed using COMSTAT (Heydorn et al., 2000).

Intracellular c-di-GMP Extraction and Analysis

The intracellular c-di-GMP was extracted according to the method reported by Spangler et al. (2010). Briefly, the bacterial cells were cultured in 12-well plates to the late exponential growth phase under the same conditions as described above and harvested (5 ml culture volume) by

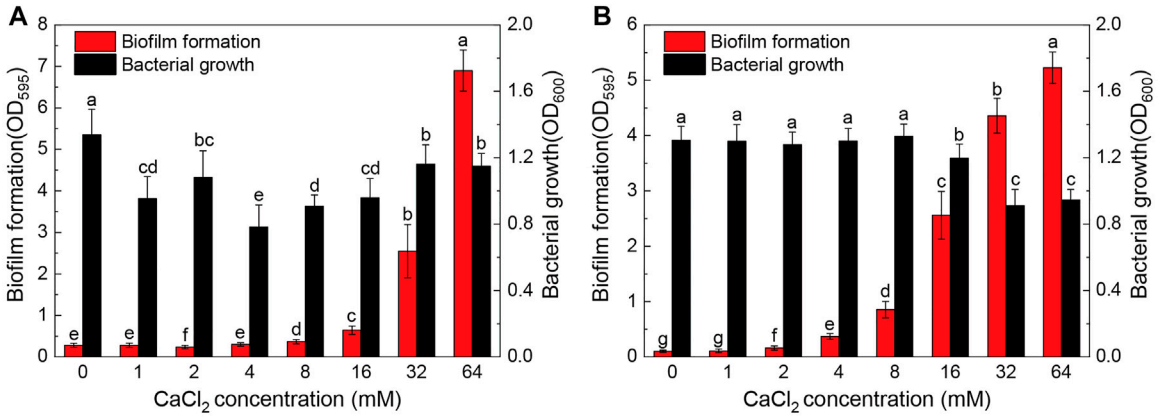

FIGURE 1 | Biofilm formation and bacterial growth of *Pseudomonas* sp. ZX01 **(A)** and *Arthrobacter* sp. ZX07 **(B)** in 12-well microtiter plates when adding different concentrations of $CaCl_2$ into the medium. Bars represented mean ± standard deviation. Different lowercase letters labeled on the bars represented the significant difference ($p < 0.05$) according to the one-way ANOVA and multiple comparisons.

immediate centrifugation at 4°C for the subsequent extraction. For each culture, the extraction was performed in triplicate. The relative quantitative analysis of c-di-GMP was conducted using a Dionex Ultimate 3000 UPLC system coupled to a TSQ Quantiva Ultra triple-quadrupole mass spectrometer (Thermo Scientific, United States). Moreover, 1 ml of the bacterial culture was collected and the cell pellet obtained by centrifugation was dissolved in 800 µl of 0.1 M NaOH. After being heat-treated at 95°C for 15 min, the protein content in the solution was determined using a BCA Protein Assay Kit. The final concentration of c-di-GMP (relative content) was normalized as peak area per mg of bacterial protein and presented as the ratio to the control group.

Statistical Analysis

All the experimental data in figures or tables were presented in the form of mean ± standard deviation. One-way ANOVA and multiple comparisons were also performed using SPSS software (V19.0; IBM, United States) to illustrate the results of different experimental conditions (i.e., Ca^{2+} concentrations). The appropriate statistical test method was selected from Fisher's LSD test and Tamhane's T2 test for multiple comparisons according to the homogeneity of variance. In general, a *p*-value of <0.05 was regarded as significantly different.

RESULTS

Effects of Calcium on Biofilm Formation

The biofilm formation and planktonic bacterial growth in the presence of different concentrations of Ca^{2+} (0–64 mM) were monitored using the microtiter plate assay. As shown in **Figure 1A**, calcium, when added at sufficient concentration, and significantly promoted biofilm formation of *Pseudomonas* sp. ZX01. In the range of 0–8 mM, Ca^{2+} had little effect on the biofilm formation; while in the range of 16–64 mM, the biofilm biomass was increased sharply in a concentration-dependent manner. The maximum amount of biofilm biomass was observed in the presence of 64 mM Ca^{2+}, which was 24.7 times that of the control (0 mM Ca^{2+}). However, the addition of Ca^{2+} reduced the planktonic bacterial growth of ZX01 by 13.3–41.6%, and the minimum bacterial density was found in the presence of 4 mM Ca^{2+}. Significantly increased biofilm formation by *Arthrobacter* sp. ZX07 was observed in the presence of exogenous calcium at a much lower Ca^{2+} concentration (2 mM) (**Figure 1B**); in addition, when Ca^{2+} concentration increased from 2 to 64 mM, the biofilm biomass increased in a more even manner; the biofilm biomass of ZX07 at 16, 32, and 64 mM Ca^{2+} was 24.4, 42.2, and 50.8 times as that of the control. These results indicated that calcium had a stronger promoting effect on ZX07 than ZX01. Furthermore, Ca^{2+} did not affect the planktonic growth of ZX07 at concentrations up to 8 mM but repressed planktonic growth by 8.4–30.2% at higher concentrations (16–64 mM).

The effect of Ca^{2+} on biofilm formation can be clearly seen in digital photos of the 12-well microtiter plates (**Figure 2**). **Figure 2A** shows that ZX01 formed more biofilms at the center of the well bottom surface in the presence of 32 mM Ca^{2+}; when Ca^{2+} concentration increased to 64 mM, the biofilms occupied the whole bottom of the wells, and the liquid/air/well wall 3-phase interface. Unlike ZX01, in the presence of 16, 32, and 64 mM Ca^{2+}, the biofilms of ZX07 mainly appeared at the edge of the well bottom rather than the center (**Figure 2B**).

Effects of Calcium on Bacterial Initial Attachment

The effects of calcium on bacterial initial attachment were determined by measuring cell attachment on glass slides. **Figure 3** presents the number of viable bacterial cells attached to the surface of the glass slide in 1 h. For *Pseudomonas* sp. ZX01, the highest initial attachment was

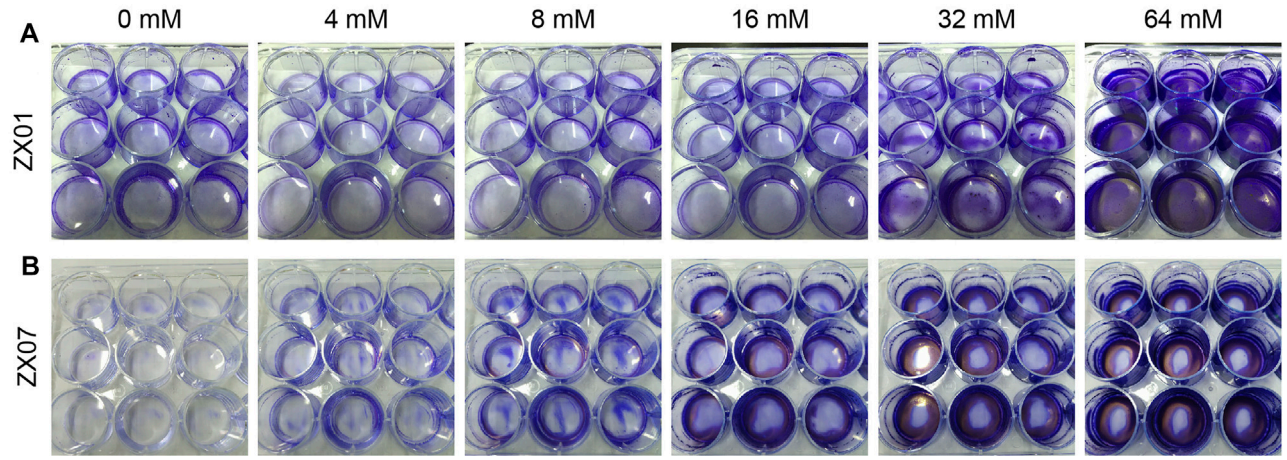

FIGURE 2 | Digital photos of biofilms formed in 12-well microtiter plates by *Pseudomonas* sp. ZX01 **(A)** and *Arthrobacter* sp. ZX07 **(B)** when adding different concentrations of $CaCl_2$ into the medium. Cells in biofilms were stained using 0.1% crystal violet.

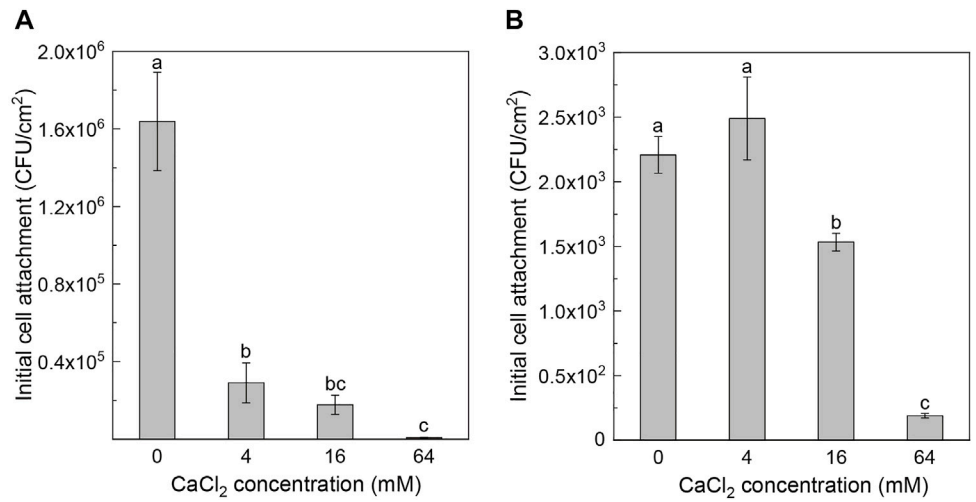

FIGURE 3 | Effects of adding $CaCl_2$ on the initial cell attachment of *Pseudomonas* sp. ZX01 **(A)** and *Arthrobacter* sp. ZX07 **(B)** on glass substrate under shaking conditions. Bars represented mean ± standard deviation. Different lowercase letters labeled on the bars represented the significant difference ($p < 0.05$) according to the one-way ANOVA and multiple comparisons.

found in the absence of Ca^{2+}, which was 1.64×10^6 CFU/cm^2 (**Figure 3A**). With increasing concentration of Ca^{2+}, the initial attachment of ZX01 was significantly repressed; the initial cell attachment in the presence of 64 mM Ca^{2+} (8.36×10^3 CFU/cm^2) was two orders of magnitude lower than that of the control. As shown in **Figure 3B**, the initial attachment of *Arthrobacter* sp. ZX07 at 0 and 4 mM Ca^{2+} was significantly higher than that at 16 and 64 mM Ca^{2+}. The lowest initial attachment was observed at a Ca^{2+} concentration of 64 mM (1.89×10^2 CFU/cm^2), which was an order of magnitude lower than that of the control (2.21×10^3 CFU/cm^2). These results indicated that Ca^{2+} can inhibit the initial attachment of the two bacterial strains to positive-charged glass surfaces.

Effects of Calcium on EPS Expressions of Biofilm Cells and Planktonic Cells

The EPS composition of biofilm cells and planktonic cells in the presence of different concentrations of calcium was chemically analyzed. As presented in **Figure 4A**, both PN and PS content in the biofilm EPS of *Pseudomonas* sp. ZX01 responded to exogenous Ca^{2+} in a significant decreasing trend. Compared with the control, 16 and 32 mM Ca^{2+} could reduce the PN

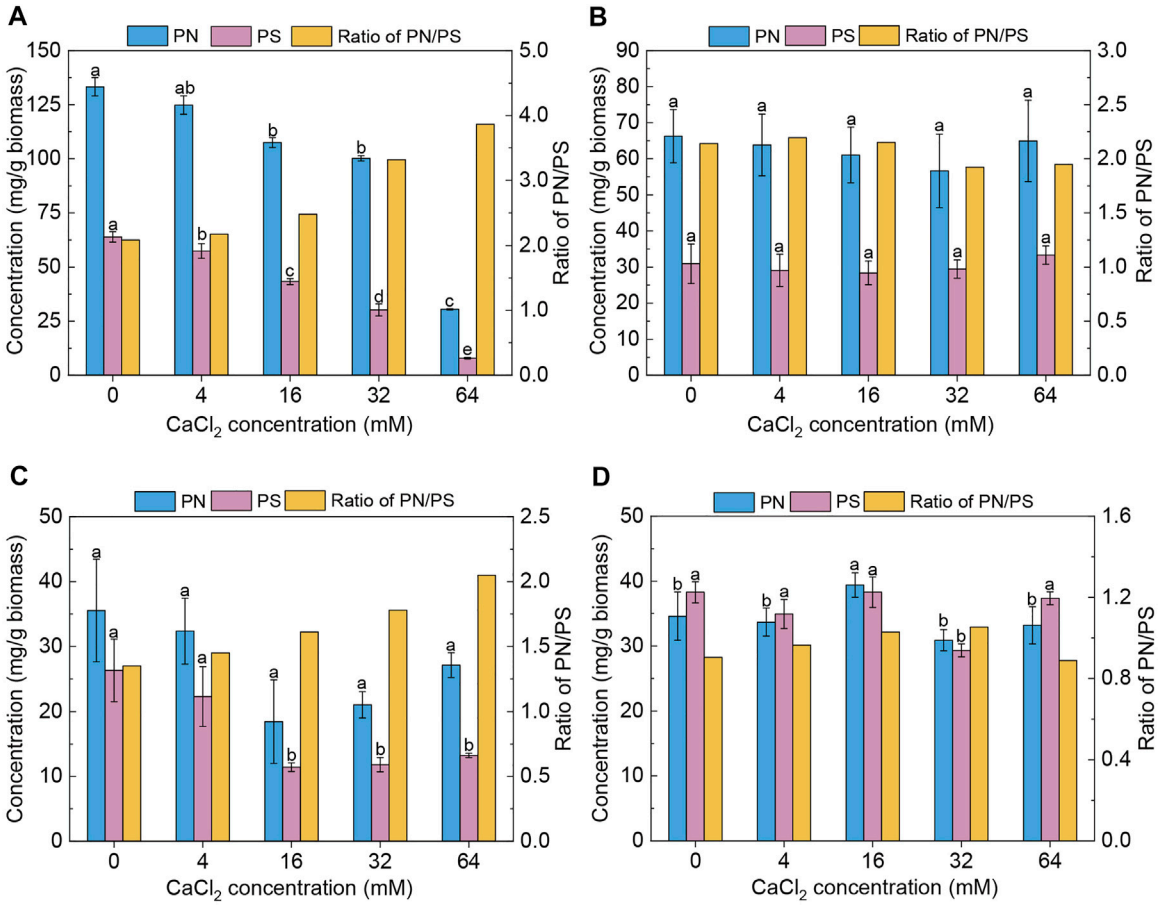

FIGURE 4 | Effects of adding $CaCl_2$ on protein (PN) content, polysaccharide (PS) content, and the ratio of protein to polysaccharide (PN/PS) in the EPS of both biofilms and planktonic cells. **(A,B)** Biofilms and planktonic cells of *Pseudomonas* sp. ZX01 **(C,D)** Biofilms and planktonic cells of *Arthrobacter* sp. ZX07. Bars represented mean ± standard deviation of three replicates. Different lowercase letters labeled on the bars represented the significant difference ($p < 0.05$) according to the one-way ANOVA and multiple comparisons.

content by 19.4 and 24.8%, respectively; while in the presence of 64 mM Ca^{2+}, the PN content (i.e., 30.5 mg/g biomass) was reduced even more sharply by 77.1%. Similarly, the PS content was decreased by 10.2–87.7% in a monotonic manner with the addition of Ca^{2+}. The PN/PS ratio of biofilm EPS increased notably (from 2.08 to 3.87) in response to exogenous calcium. Nevertheless, the PN and PS content in the EPS of planktonic bacterial cells were practically unaffected by the addition of Ca^{2+}, staying at around 65 and 30 mg/g biomass, respectively (**Figure 4B**). Regarding *Arthrobacter* sp. ZX07, the change in PN content in biofilm EPS (**Figure 4C**) was not statistically significant. However, high Ca^{2+} concentrations (16, 32, and 64 mM) reduced the PS content by 49.8–56.5%. Consequently, the PN/PS ratio of ZX07 biofilm EPS increased from 1.35 (the control) to 2.04 (64 mM Ca^{2+}) with increasing Ca^{2+} concentrations. Like ZX01, the EPS components of planktonic ZX07 cells were not influenced by Ca^{2+} (**Figure 4D**).

EEM fluorescence spectra were obtained to characterize the EPS composition. In general, EEM spectra could be divided into five regions: Regions I and II represent aromatic protein-like compounds; Region III represents fulvic acid-like compounds; Region IV represents microbial products such as tyrosine-like, tryptophan-like, and protein-like compounds; Region V represents humic acid-like compounds (Chen et al., 2003). Interestingly, the EEM peaks of the biofilm EPS and planktonic EPS in the absence or presence of Ca^{2+} are similar (**Figures 5A–D**), indicating that Ca^{2+} did not affect the compounds in EPS of *Pseudomonas* sp. ZX01. Specifically, the two peaks identified from the EEMs were EX/EM = 225/325 nm (Region I) and EX/EM = 275/325 nm (Region IV). In contrast, Ca^{2+} had remarkable influences on the EPS composition of *Arthrobacter* sp. ZX07. Without adding Ca^{2+}, there were 3 peaks in the EEMs of both biofilm and planktonic EPS (**Figures 5E,G**): EX/EM = 220/350 nm (Region II), EX/EM = 280/350 nm (Region IV), and EX/EM = 325/390 nm (Region V). However, despite sharing the same two peaks in Region II and Region IV, the EEMs of biofilm EPS in the presence of 64 mM Ca^{2+} presented two different peaks locating at EX/EM = 360/450 nm (Region V), and EX/EM = 270/450 nm (Region V) (**Figure 5F**). Additionally, a different peak at EX/EM = 350/

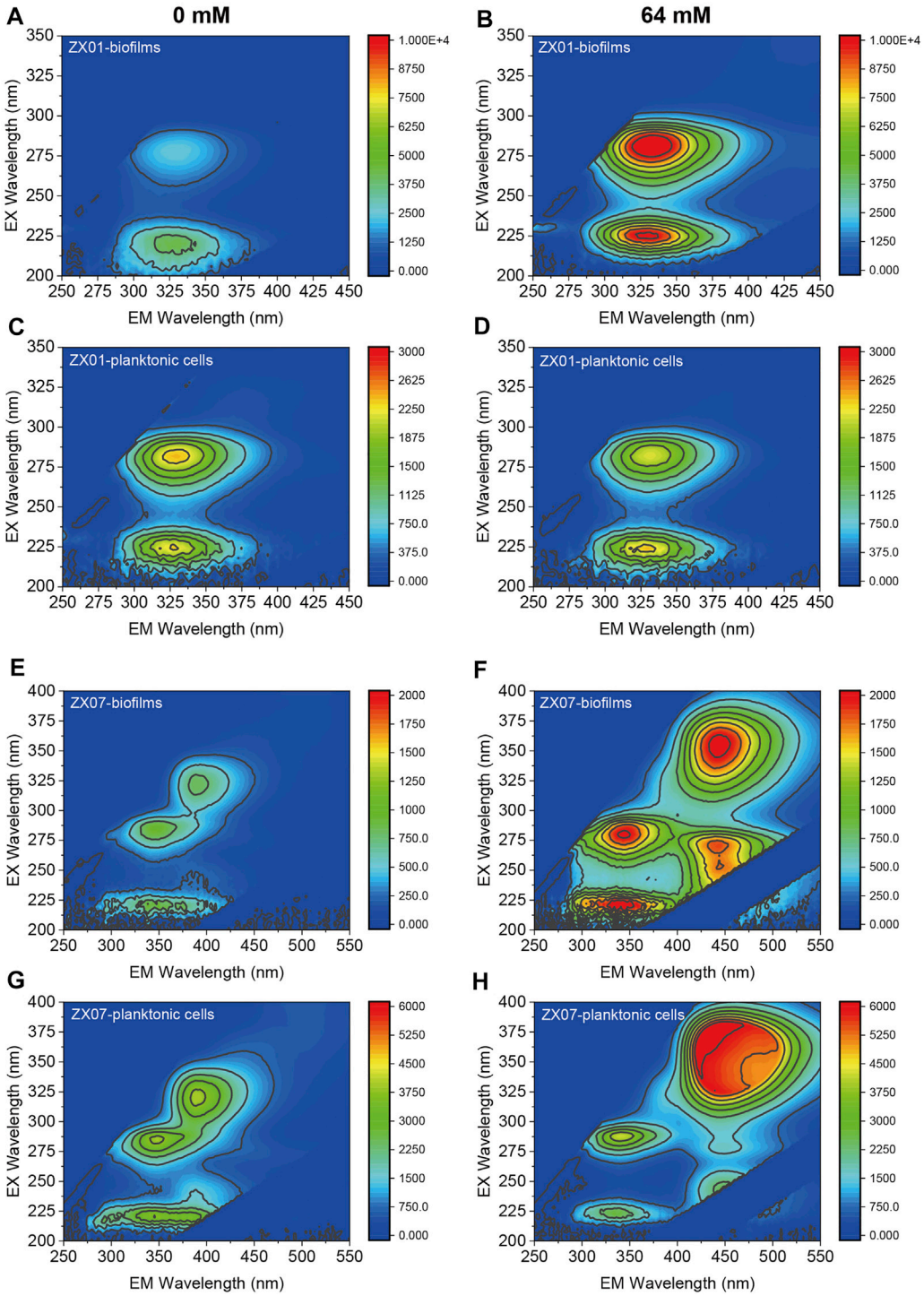

FIGURE 5 | EEM fluorescence spectra of the EPS produced by both biofilms and planktonic cells. **(A,B)** Biofilms of *Pseudomonas* sp. ZX01 in the presence of 0 and 64 mM of $CaCl_2$ **(C,D)** Planktonic cells of *Pseudomonas* sp. ZX01 in the presence of 0 and 64 mM of $CaCl_2$. **(E,F)** Biofilms of *Arthrobacter* sp. ZX07 in the presence of 0 and 64 mM of $CaCl_2$ **(G,H)** Planktonic cells of *Arthrobacter* sp. ZX07 in the presence of 0 and 64 mM of $CaCl_2$.

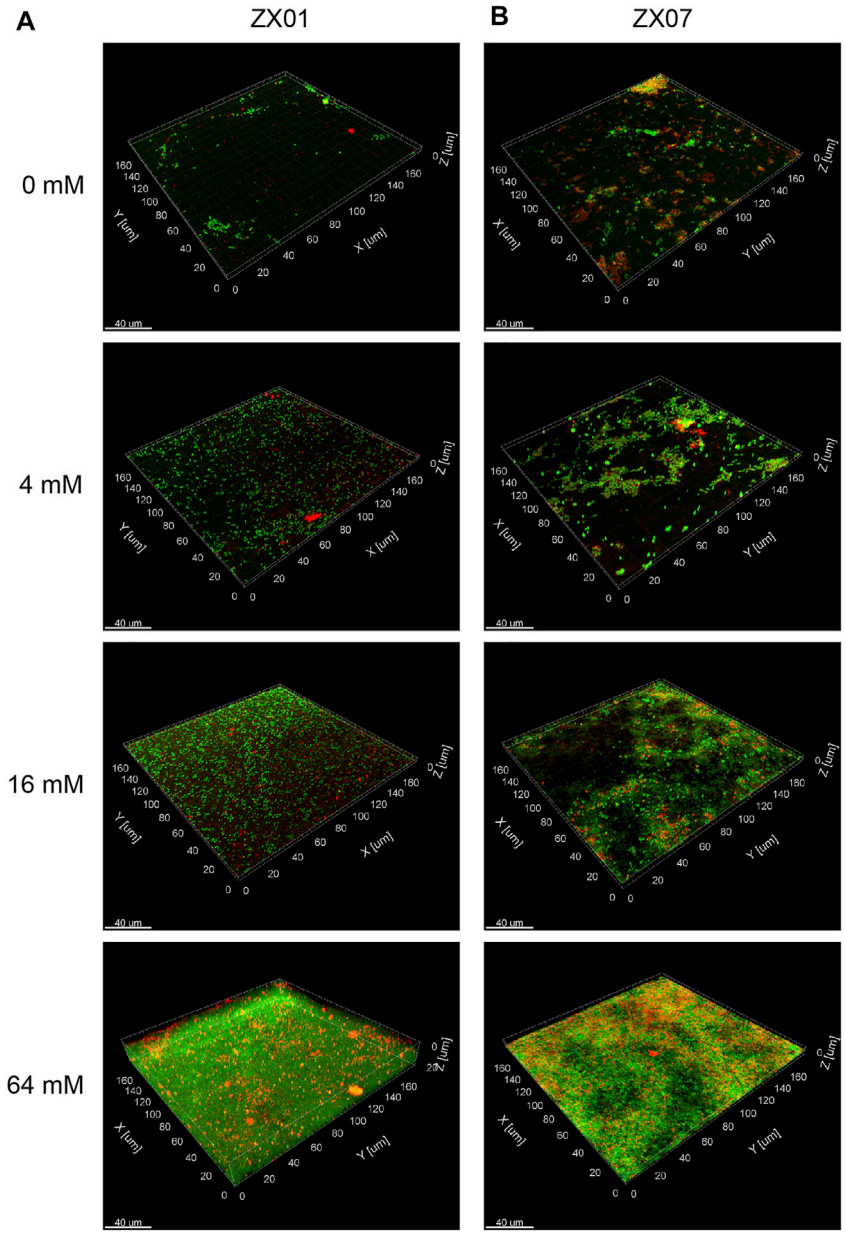

FIGURE 6 | CLSM 3-D images of the biofilms formed by *Pseudomonas* sp. ZX01 **(A)** and *Arthrobacter* sp. ZX07 **(B)** in the presence of 0, 4, 16, and 64 mM of $CaCl_2$. The cells were stained green with SYTO9; the polysaccharides were stained red with conA-T; the yellow fluorescence represented the combination of cells and polysaccharides.

450 nm (Region V) appeared in the EEMs of planktonic EPS at 64 mM Ca^{2+} (**Figure 5H**). The above results suggested that exogenous calcium promoted ZX07 to produce certain humic acid-like compounds.

Effects of Calcium on Biofilm Architecture

The architecture and topography of the biofilms of the two pyridine-degrading bacteria, formed on μ-Slide surfaces in 24 h, were examined by CLSM 3-D imaging (**Figure 6**). The green fluorescence signal represents bacterial cells, and the red signal represents PS in EPS. In the absence of Ca^{2+}, few ZX01 cells adhered to the substrate and formed small aggregates (**Figure 6A**). Quantitative analysis of CLSM images (**Table 1**) showed very low average thickness and coverage of ZX01 biofilms at 2.06 ± 0.29 μm and 12.64%, respectively. At Ca^{2+} concentrations of 4 and 16 mM, many more ZX01 cells adhered to the surfaces and the cells were uniformly distributed; PS became clearly visible in biofilms. As a result, the surface coverage of ZX01 biofilms at 4 and 16 mM Ca^{2+} went up to 25.17 and 42.09%, respectively (**Table 1**). Intriguingly, when

TABLE 1 | Characteristics of biofilms formed by ZX01 and ZX07 under different calcium concentrations calculated from the CLSM images using COMSTAT.

Groups	Total biomass ($\mu m^3/\mu m^2$)	Average thickness (μm)	Average coverage (%)	Surface to biovolume ratio ($\mu m^2/\mu m^3$)	Roughness coefficient	Average colony size (μm^2)
ZX01-0 mM	0.57 ± 0.06^{b}	2.06 ± 0.29^{c}	12.64 ± 0.26^{d}	12.39 ± 0.66^{a}	0.44 ± 0.08^{a}	10.92 ± 3.53^{b}
ZX01-4 mM	0.97 ± 0.25^{b}	2.41 ± 0.36^{bc}	25.17 ± 6.38^{c}	8.10 ± 1.05^{b}	0.23 ± 0.09^{b}	12.37 ± 2.82^{b}
ZX01-16 mM	1.68 ± 0.44^{b}	3.17 ± 0.41^{b}	42.09 ± 7.40^{b}	5.31 ± 0.78^{c}	0.13 ± 0.03^{c}	14.41 ± 2.96^{b}
ZX01-64 mM	16.49 ± 0.63^{a}	19.56 ± 1.90^{a}	75.75 ± 3.42^{a}	1.07 ± 0.11^{d}	0.02 ± 0.01^{d}	217.30 ± 55.09^{a}
ZX07-0 mM	0.40 ± 0.21^{c}	0.78 ± 0.35^{c}	9.13 ± 3.26^{c}	7.86 ± 1.81^{a}	1.25 ± 0.24^{a}	13.40 ± 3.73^{d}
ZX07-4 mM	0.65 ± 0.27^{bc}	1.17 ± 0.34^{bc}	15.47 ± 5.62^{bc}	5.21 ± 2.42^{b}	1.19 ± 0.24^{a}	28.13 ± 4.64^{c}
ZX07-16 mM	0.97 ± 0.11^{b}	1.73 ± 0.18^{b}	20.40 ± 3.99^{b}	3.87 ± 0.68^{bc}	0.58 ± 0.03^{b}	39.60 ± 2.38^{b}
ZX07-64 mM	3.75 ± 0.40^{a}	6.06 ± 0.92^{a}	52.09 ± 7.93^{a}	2.02 ± 0.32^{c}	0.13 ± 0.02^{c}	84.11 ± 7.93^{a}

Note: The data were presented as mean ± standard deviation (n = 6). Different lowercase letters labeled on the data represented the significant difference ($p < 0.05$) according to the one-way ANOVA, and Tamhane's T2 or LSD, post-tests.

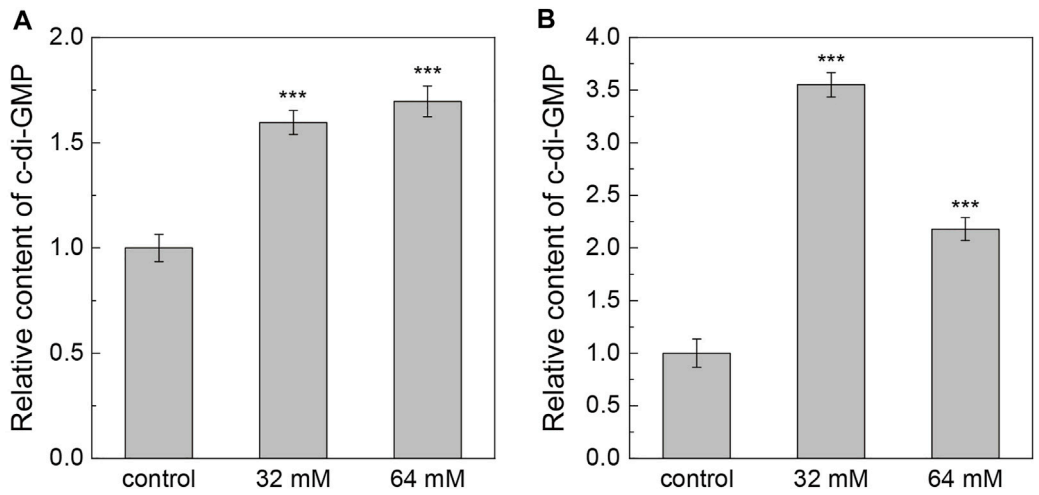

FIGURE 7 | Effects of adding $CaCl_2$ on the relative content of intracellular c-di-GMP of *Pseudomonas* sp. ZX01 **(A)** and *Arthrobacter* sp. ZX07 **(B)**. Bars represented mean ± standard deviation of three replicates. Symbols (***) labeled on the bars represented the significant difference ($p < 0.001$) with the control according to Student's t tests.

64 mM Ca^{2+} was added, ZX01 formed dense and thick biofilms, in which the cells and EPS were distributed in a well-structured mode. The total biomass, average thickness, average coverage, and average colony size of ZX01 biofilms in this condition were all elevated by several times; and the sharp reduction of surface to biovolume ratio and roughness coefficient also suggest that more bacterial cells were aggregated in the form of biofilms. Similar trends were observed in the biofilms of *Arthrobacter* sp. ZX07 (**Figure 6B**): when the concentration of exogenous Ca^{2+} increased from 0 to 16 mM, more ZX07 cells were attached to the surfaces and the microcolonies became larger, but the distribution of the cells was not uniform; in the presence of 64 mM Ca^{2+}, ZX07 developed extensive and mature biofilms, in which the cells were covered by large amounts of EPS. However, there was a notable difference in the influences of calcium on the biofilm architecture of ZX01 and ZX07. In the range of 0–16 mM, the average colony size of ZX01 biofilms was little affected by Ca^{2+}; and the cells, stimulated by Ca^{2+}, attached to the substrate in a separated pattern. In contrast, a significant increase in the average colony size was found in ZX07 biofilms, indicating that Ca^{2+} possibly promoted ZX07 cells to attach to those which had already colonized at the substrate. Therefore, it could be speculated that, for these two strains, the mechanisms inherent in the stimulatory effects of Ca^{2+} on biofilm development were different.

Effects of Calcium on c-di-GMP Level

To address whether exogenous calcium influences the expression of the second messenger c-di-GMP, we analyzed the intracellular c-di-GMP level of the two pyridine-degrading bacteria at different Ca^{2+} concentrations. As exhibited in **Figure 7A**, after culturing for 24 h, the introduction of Ca^{2+} into the medium significantly elevated the c-di-GMP level in *Pseudomonas* sp. ZX01 cells. The relative content of c-di-GMP in the presence of 32 and 64 mM Ca^{2+} was 59.5 and 69.6% higher than that of the control. In regard to *Arthrobacter* sp. ZX07, the elevation of intracellular c-di-GMP level caused by Ca^{2+} was even more remarkable (**Figure 7B**). The relative content of c-di-GMP in ZX07 cells at 32 and 64 mM Ca^{2+} was 3.55 and 2.18 times that of the control.

DISCUSSION

In this present study, the significant promotion of biofilm formation of two pyridine-degrading bacteria, *Pseudomonas* sp. ZX01 and *Arthrobacter* sp. ZX07, caused by calcium supplementation was clearly observed. Few cells of the two strains attached to the 12-well plates or μ-Slide coverslips in the absence of Ca^{2+} (**Figures 1**, **6**), indicating they harbored very poor biofilm-forming abilities in their natural state. Hence, it might affect their performances in the bioaugmented biofilm reactors. However, when exposed to Ca^{2+} of a certain concentration range (8–64 mM for ZX01 and 2–64 mM for ZX07), the biofilm biomass formed by the two strains increased greatly in a monotonic and dose-dependent pattern. Mangwani et al. (2014) also reported a dose-dependent increase of *P. mendocina* NR802 biofilms due to the Ca^{2+} addition, but the concentration tested was limited in 5–20 mM. The biofilm formation of *Sinorhizobium meliloti* was elevated in a similar manner by the addition of 7–28 mM Ca^{2+} (Rinaudi et al., 2006). While Zhou et al. (2016) found that within a much larger range of Ca^{2+} concentration (3.125–800 mM), the biofilm formation of *Citrobacter werkmanii* BF-6 was enhanced notably, but the enhancement presented a non-monotonic trend (i.e., increasing firstly and decreasing afterward). Similarly, the biofilm-forming ability of the foodborne pathogen *Cronobacter sakazakii* showed an increase and subsequent decrease with the increasing Ca^{2+} concentration from 0 to 135 mM (Ye et al., 2015). These results suggested that the sensitivity of different bacterial species in response to exogenous calcium varied. Thus, when applying the calcium-mediated regulating strategy to control bacterial biofilm formation in medical, marine, agricultural, or environmental cases, it is important to understand the effects of calcium on the specific bacterial strain of interest due to the high diversity of bacteria.

A typical bacterial biofilm formation process can be divided into five steps: 1) initial cell-to-surface attachment, 2) irreversible adhesion via producing EPS, 3) proliferation and microcolony formation, 4) maturation of biofilms with complex structures, 5) biofilm aging with the dispersal of motile cells (Stoodley et al., 2002; Armbruster and Parsek, 2018). In the first step, bacterial cells sense and attach to the surface reversibly with the assistance of cell appendages (e.g., flagellum) after overcoming the electrostatic repulsion between the cell surface and the substratum (Renner and Weibel, 2011). Our results herein revealed that the presence of Ca^{2+} in the surrounding solutions significantly repressed the initial cell attachment of both ZX01 and ZX07 to the positive-charged glass surfaces (**Figure 3**). As widely known, bacterial cell surfaces are negatively charged (Soni et al., 2008), and thus Ca^{2+}, as a divalent cation, can effectively neutralize the surface charge by interacting with ligands on the cell surfaces (Wang et al., 2019). Furthermore, in the light of electrostatic double layer compression theory, the increasing ionic strength of the solutions caused by exogenous Ca^{2+} will decrease the absolute value of the negative zeta potential of the bacteria cells (Chen and Walker, 2007; Bundeleva et al., 2011). Thus, when adding high concentrations of Ca^{2+} into the medium, the surface charge of the two bacteria would become less negative. This effect could bring both adverse and favorable consequences for initial cell-to-surface attachment, which depends on whether the surface charge of the substratum is positive or negative. For instance, another divalent cation, Mg^{2+}, was validated to exhibit a stimulatory effect on the adhesion of *Pseudomonas* sp. strain B13 to negative-charged mineral surfaces (Simoni et al., 2000). However, in the case of extremely high ionic strength caused by calcium (e.g. 1,000 mM), the adhesion efficiency of bacterial cells to quartz surfaces, which were negative-charged, and could also be reduced due to the repulsive electrostatic forces (Chen and Walker, 2007). Apart from neutralizing surface charge, Ca^{2+} has been shown to initiate strong cation bridging interactions between high-affinity sites on cell surfaces and the conditioning film of substrata, and thereby facilitating the adhesion of *P. aeruginosa* cells to alginate-conditioned quartz surfaces (de Kerchove and Elimelech, 2008). Combined with our findings in the present study, it can be concluded that the impacts of Ca^{2+} on the initial cell-to-surface attachment were multi-faceted and substantially linked to physicochemical interactions, yet biological factors presumably played a minor role in this step.

During the next steps of biofilm formation, the bacterial self-secreted EPS consisting of PN, PS, nucleic acids, lipids, humic substances, etc., play more important roles in assisting cell-to-cell aggregation, and biofilm structure construction (Vu et al., 2009; Flemming and Wingender, 2010). Previous research regarding the effects of Ca^{2+} on EPS production mostly showed an enhancing impact. For example, adding an additional 10 mM Ca^{2+} in the medium could significantly promote *Bacillus* sp. cells to synthesize more PN and PS in EPS (He et al., 2016). Liu and Sun (2011) also offered evidence that the extracellular PN produced by microbial cells in sequential batch reactors increased notably when Ca^{2+} of 50 and 100 mg/L was added into the reactors, thereby enhancing bacterial aggregation to form granules. However, inconsistent with these findings, our study found that PN and PS content in biofilms formed by the two strains decreased in response to the increasing Ca^{2+} concentration (**Figure 4**), yet the biofilm biomass increased evidently. It means that in the presence of exogenous Ca^{2+}, the cells of ZX01 and ZX07 could form more biofilms but require lower EPS production for each bacterial cell. In other words, a smaller amount of EPS would support larger biofilm structures with the assistance of Ca^{2+}. This may be attributed to the cation bridge effect, i.e., Ca^{2+} can bind to the negatively charged functional groups in EPS, and consequently forming EPS-Ca^{2+}-EPS bridges, which favors the construction of sophisticated biofilm structures (Sobeck and Higgins, 2002; Liu and Sun, 2011; Wang et al., 2019). In particular, functional groups such as carboxylic acid and phosphates in extracellular PS were known binding sites for Ca^{2+} (Astasov-Frauenhoffer et al., 2017); more recently, cationic bridging by Ca^{2+} between eDNA was also reported, which promoted bacterial aggregation and biofilm development of several strains including *P. aeruginosa* and *S. aureus* (Das et al., 2014). Therefore, the amount of EPS production per cell may not be a good predictor of the resulting biofilm biomass; Ca^{2+}-mediated interactions among microbial cells and EPS can be highly efficient in forming a large biofilm structure.

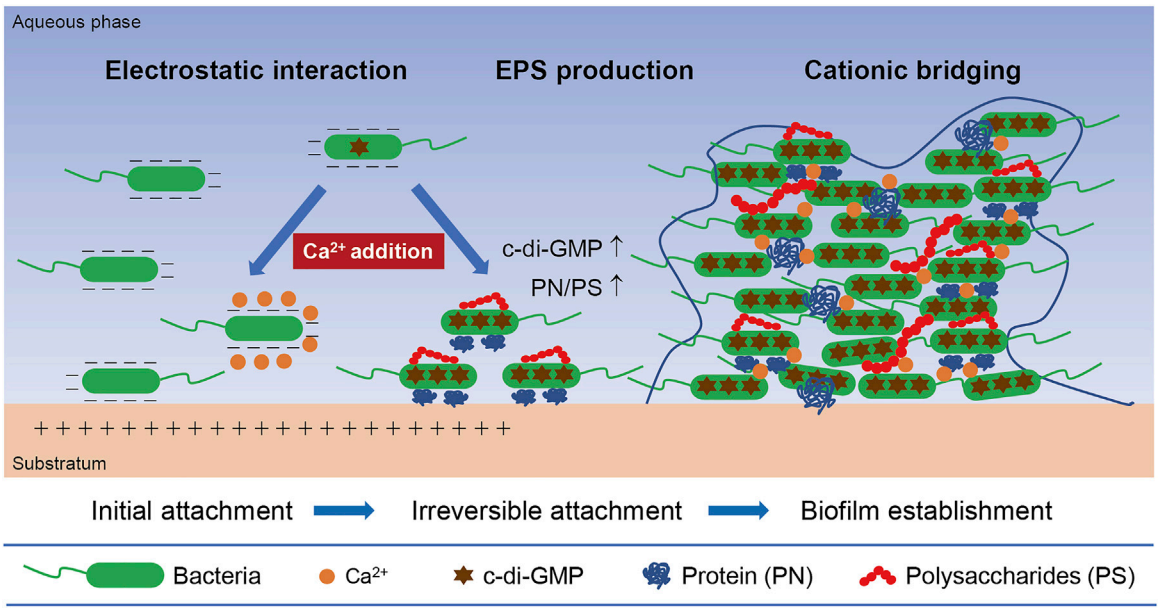

FIGURE 8 | A conceptual illustration of the mechanisms inherent in the calcium-mediated regulation on bacterial biofilm formation.

The ratio of PN/PS in EPS is widely regarded as an important indicator of microbial cell-to-cell aggregating ability in biofilm or granular sludge formation processes. A higher PN content elevates the hydrophobicity of cell surfaces, thereby inducing strong hydrophobic interaction between microbial cells (Hou et al., 2015; Zhao Y. et al., 2018). Our experiments found that the PN/PS ratio in the biofilm EPS of ZX01 and ZX07 increased greatly in the presence of Ca^{2+} (**Figure 4**). This suggests that calcium-mediated promotion of biofilm formation of these two strains can also be attributed to the higher PN/PS ratio in EPS in addition to the cationic bridging effect of Ca^{2+}. Furthermore, the regulatory effects of Ca^{2+} on multiple gene expressions and metabolic activities have been noted by many studies. Parker et al. (2016) indicated that exogenous Ca^{2+} could induce a substantial transcriptional alteration of the bacterial plant pathogen *Xylella fastidiosa*, including genes encoding cell attachment, motility, and PS secretion, which facilitated biofilm development. The supplementation of 400 mM Ca^{2+} also resulted in a more complex protein expression mode in both biofilms and planktonic cells of *C. werkmanii* BF-6 (Zhou et al., 2016). As demonstrated using EEM fluorescence spectra in our study, 64 mM Ca^{2+} caused a remarkable impact on the EPS expressions in both biofilms, and planktonic cells of ZX07, i.e., the production of humic acid-like compounds, while no significant changes were observed in those of ZX01. Past research has mentioned that due to the abundant ionizable functional groups such as carboxyl and phenolic hydroxyl, humic substances showed high affinities to interact with metal ions (e.g. Cu^{2+}, Ca^{2+}) and form complexes (Wang et al., 2015; Zhao et al., 2020). Hence, the occurrence of humic acid-like compounds in EPS might favor the formation of EPS-Ca^{2+}-EPS bridges and elevate the biofilm-forming ability of ZX07.

The morphological phenotypes of mature biofilms were also altered by Ca^{2+}-mediated regulation. As shown in the CLSM images and the COMSTAT analysis (**Figure 6**; **Table 1**), for both ZX01 and ZX07 biofilms, the increase of total biomass, average thickness, and average coverage, and the decrease of roughness coefficient were ascertained in response to the increasing Ca^{2+} concentration, consistent the results in other bacterial strains like *C. werkmanii* and *Shewanella oneidensis* (Zhou et al., 2016; Zhang et al., 2019). Interestingly, the average colony size of ZX01 and ZX07 exhibited quite different responses to the supplementary Ca^{2+} of relatively lower concentrations (i.e., 4 and 16 mM). Specifically, the microcolonies of ZX01 were more dispersed and homogeneous, while ZX07 unevenly developed its microcolonies which were like "rugged mountains". To the best of our knowledge, this discrepancy might be attributed to the flagella-mediated motility. According to the SEM images of the two strains (**Supplementary Figure S1**), ZX01 possesses a cellular accessory structure resembling a polar flagellum, while the cell surface of ZX07 is quite smooth without any appendages. In addition, as verified using the motility tests, ZX01 had much stronger swimming motility and swarming motility, both propelled by flagella, than ZX07 (**Supplementary Figure S2, S3**). Existing evidence demonstrated that bacteria with higher motility tend to be more proficient in moving at the solid-liquid interface and attaching to an abiotic surface (O'Toole and Kolter, 1998; Van Houdt and Michiels, 2005), which was crucial in biofilm development. Therefore, with the assistance of flagella-mediated motility, ZX01 could migrate freely at the substratum and attach onto more sites of the surface, thereby producing more homogeneous biofilms facilitated by Ca^{2+}; whereas the moving area of ZX07 was limited, and they tended to form microcolonies clinging to the cells that attached randomly to the surface, thus resulting in mountain-like biofilms. Moreover, the biofilm-

forming positions of the two strains were also different (**Figure 2**), which might be still owing to their discrepant motilities. Hence, under the hydraulic shear force in the rotary 12-well plates, ZX01 cells with high motility were able to occupy the whole bottom to form biofilms, yet ZX07 cells with low motility were forced to settle at the periphery of the bottom. Taken together, it was inferred that Ca^{2+} and cell motility might exert a joint regulatory effect on bacterial biofilm formation. Regardless of cell motility, Ca^{2+} can indeed promote the bacteria to form more biofilms, but the motility still exerts influences upon the biofilm architecture.

Recently, the intracellular messenger c-di-GMP was found in many studies to play a global role in regulating the switch of bacterial lifestyle from planktonic state to biofilm-associated state (Valentini and Filloux, 2016; Jenal et al., 2017). By binding to various specific proteins (namely, effectors) in bacterial cells, c-di-GMP controls a wide range of cellular processes including virulence, motility, EPS production, biofilm formation, and dispersion, etc. (Chen et al., 2012). In particular, the intracellular level of c-di-GMP, which is the result of the synthesis by diguanylate cyclases (DGCs) and the degradation by phosphodiesterases (PDEs), is positively associated with the biofilm-forming tendency of bacteria (Ha and O'Toole, 2015). Herein, our study shows elevated intracellular c-di-GMP levels in both ZX01 and ZX07 in the presence of supplementary Ca^{2+}, which was accompanied by enhanced biofilm formation (**Figure 7**). This seems to suggest a potential correlation between Ca^{2+} and c-di-GMP production, although few prior studies have found similar results. Parker et al. (2016) found that the expression of a gene involved in the synthesis of c-di-GMP, *cgsA*, in *X. fastidiosa*, exhibited a weak but non-significant increase in the presence of 4 mM Ca^{2+}. Given the fact that Ca^{2+} is also an essential second messenger in bacterial cells (Dominguez et al., 2015), the little-known interaction of Ca^{2+} and c-di-GMP needs to be further investigated.

In summary, a proposed mechanism of the calcium-mediated regulation on the biofilm formation of the two pyridine-degrading bacteria was illustrated in **Figure 8**. Typically, bacterial cell-to-surface adhesion is driven by the electrostatic interaction, thus the negative-charged bacterial cells tend to adhere to a positive-charged material surface. The divalent Ca^{2+} can neutralize the surface charge of bacterial cells and further weaken their initial attachment to the positive-charged substratum. However, in the presence of Ca^{2+}, the EPS composition of biofilms can be significantly altered, resulting in a higher PN/PS ratio which facilitates the irreversible attachment between bacterial cells. EPS-Ca^{2+}-EPS bridges induced by exogenous calcium also increase the efficiency of EPS in binding cells and constructing biofilm structures. Moreover, the elevated intracellular c-di-GMP level is validated to account for the promotion of biofilm formation.

CONCLUSION

This study comprehensively investigated the effects of Ca^{2+} on different biofilm developing stages of two newly isolated pyridine-degrading bacteria. The main conclusions are as follows: 1) the supplemented Ca^{2+} of 16–64 mM markedly promoted the biofilm formation of the two strains with insufficient biofilm-forming capacities; 2) by altering cell surface charge, Ca^{2+} influenced the initial cell-to-surface attachment of the two strains in the first step of biofilm formation; 3) in the presence of Ca^{2+}, the relatively lower EPS production per cell in biofilms could bind more biofilm biomass, presumably attributed to the cationic bridging between Ca^{2+} and EPS; 4) the ratio of PN/PS in biofilm EPS of the two strains showed an increasing tendency in response to exogenous Ca^{2+}, which favored cell aggregation and biofilm formation; 5) the intracellular c-di-GMP levels were elevated notably by the supplementary Ca^{2+}, thereby driving the switch of the two strains from planktonic lifestyle to biofilm lifestyle. Collectively, these findings demonstrated the promising feasibility of facilitating bacterial biofilm formation onto engineering carriers with a Ca^{2+}-based manipulation strategy, which will provide valuable guidance for the application of these pyridine-degrading strains into bioaugmented reactors.

DATA AVAILABILITY STATEMENT

The datasets presented in this study can be found in online repositories. The names of the repository/repositories and accession number(s) can be found in the article/**Supplementary Material**.

AUTHOR CONTRIBUTIONS

Conceptualization: FX and DW; Methodology: FX and QL; Formal analysis and investigation: FX; Writing—original draft preparation: FX; Writing—review and editing: DW and QL; Funding acquisition: DW and QL.

FUNDING

This study was financially supported by the National Natural Science Foundation of China (Grant number 51938001 and 51529801).

ACKNOWLEDGMENTS

The authors would like to acknowledge Institutional Center for Shared Technologies and Facilities, Institute of Microbiology, Chinese Academy of Sciences and Tsinghua University Branch of China National Center for Protein Sciences (Beijing) for infrastructural support.

SUPPLEMENTARY MATERIAL

The Supplementary Material for this article can be found online at: https://www.frontiersin.org/articles/10.3389/fenvs.2022.815528/full#supplementary-material

REFERENCES

Armbruster, C. R., and Parsek, M. R. (2018). New Insight into the Early Stages of Biofilm Formation. *Proc. Natl. Acad. Sci. USA* 115 (17), 4317–4319. doi:10.1073/pnas.1804084115

Astasov-Frauenhoffer, M., Varenganayil, M. M., Decho, A. W., Waltimo, T., and Braissant, O. (2017). Exopolysaccharides Regulate Calcium Flow in Cariogenic Biofilms. *Plos One* 12 (10), e0186256. doi:10.1371/journal.pone.0186256

Bai, Y., Sun, Q., Xing, R., Wen, D., and Tang, X. (2010). Removal of Pyridine and Quinoline by Bio-Zeolite Composed of Mixed Degrading Bacteria and Modified Zeolite. *J. Hazard. Mater.* 181 (1–3), 916–922. doi:10.1016/j.jhazmat.2010.05.099

Bai, Y., Sun, Q., Zhao, C., Wen, D., and Tang, X. (2009). Aerobic Degradation of Pyridine by a New Bacterial Strain, Shinella Zoogloeoides BC026. *J. Ind. Microbiol. Biotechnol.* 36 (11), 1391–1400. doi:10.1007/s10295-009-0625-9

Bai, Y., Sun, Q., Zhao, C., Wen, D., and Tang, X. (2008). Microbial Degradation and Metabolic Pathway of Pyridine by a Paracoccus Sp. Strain BW001. *Biodegradation* 19 (6), 915–926. doi:10.1007/s10532-008-9193-3

Bi, E., Schmidt, T. C., and Haderlein, S. B. (2006). Sorption of Heterocyclic Organic Compounds to Reference Soils: Column Studies for Process Identification. *Environ. Sci. Technol.* 40 (19), 5962–5970. doi:10.1021/es060470e

Bilecen, K., and Yildiz, F. H. (2009). Identification of a Calcium-Controlled Negative Regulatory System AffectingVibrio Choleraebiofilm Formation. *Environ. Microbiol.* 11 (8), 2015–2029. doi:10.1111/j.1462-2920.2009.01923.x

Bourven, I., Joussein, E., and Guibaud, G. (2011). Characterisation of the Mineral Fraction in Extracellular Polymeric Substances (EPS) from Activated Sludges Extracted by Eight Different Methods. *Bioresour. Technol.* 102 (14), 7124–7130. doi:10.1016/j.biortech.2011.04.058

Bundeleva, I. A., Shirokova, L. S., Bénézeth, P., Pokrovsky, O. S., Kompantseva, E. I., and Balor, S. (2011). Zeta Potential of Anoxygenic Phototrophic Bacteria and Ca Adsorption at the Cell Surface: Possible Implications for Cell protection from CaCO3 Precipitation in Alkaline Solutions. *J. Colloid Interf. Sci.* 360 (1), 100–109. doi:10.1016/j.jcis.2011.04.033

Cai, W., De La Fuente, L., and Arias, C. R. (2019). Transcriptome Analysis of the Fish Pathogen Flavobacterium Columnare in Biofilm Suggests Calcium Role in Pathogenesis. *BMC Microbiol.* 19, 151. doi:10.1186/s12866-019-1533-4

Chen, G., and Walker, S. L. (2007). Role of Solution Chemistry and Ion Valence on the Adhesion Kinetics of Groundwater and marine Bacteria. *Langmuir* 23 (13), 7162–7169. doi:10.1021/la0632833

Chen, W., Westerhoff, P., Leenheer, J. A., and Booksh, K. (2003). Fluorescence Excitation–Emission Matrix Regional Integration to Quantify Spectra for Dissolved Organic Matter. *Environ. Sci. Technol.* 37 (24), 5701–5710. doi:10.1021/es034354c

Chen, Y., Chai, Y., Guo, J.-h., and Losick, R. (2012). Evidence for Cyclic Di-GMP-Mediated Signaling in Bacillus Subtilis. *J. Bacteriol.* 194 (18), 5080–5090. doi:10.1128/Jb.01092-12

Das, T., Sehar, S., Koop, L., Wong, Y. K., Ahmed, S., Siddiqui, K. S., et al. (2014). Influence of Calcium in Extracellular DNA Mediated Bacterial Aggregation and Biofilm Formation. *PLOS ONE* 9 (3), e91935. doi:10.1371/journal.pone.0091935

de Kerchove, A. J., and Elimelech, M. (2008). Calcium and Magnesium Cations Enhance the Adhesion of Motile and Nonmotile *Pseudomonas A* on Alginate Films. *Langmuir* 24 (7), 3392–3399. doi:10.1021/la7036229

Domínguez, D. C., Guragain, M., and Patrauchan, M. (2015). Calcium Binding Proteins and Calcium Signaling in Prokaryotes. *Cell Calcium* 57 (3), 151–165. doi:10.1016/j.ceca.2014.12.006

Dubois, M., Gilles, K. A., Hamilton, J. K., Rebers, P. A., and Smith, F. (1956). Colorimetric Method for Determination of Sugars and Related Substances. *Anal. Chem.* 28 (3), 350–356. doi:10.1021/ac60111a017

Flemming, H.-C., Wingender, J., Szewzyk, U., Steinberg, P., Rice, S. A., and Kjelleberg, S. (2016). Biofilms: An Emergent Form of Bacterial Life. *Nat. Rev. Microbiol.* 14, 563–575. doi:10.1038/nrmicro.2016.94

Flemming, H.-C., and Wingender, J. (2010). The Biofilm Matrix. *Nat. Rev. Microbiol.* 8 (9), 623–633. doi:10.1038/nrmicro2415

Flemming, H.-C., and Wuertz, S. (2019). Bacteria and Archaea on Earth and Their Abundance in Biofilms. *Nat. Rev. Microbiol.* 17 (4), 247–260. doi:10.1038/s41579-019-0158-9

Fu, S., Fan, H., Liu, S., Liu, Y., and Liu, Z. (2009). A Bioaugmentation Failure Caused by Phage Infection and Weak Biofilm Formation Ability. *J. Environ. Sci.* 21 (8), 1153–1161. doi:10.1016/S1001-0742(08)62396-7

Gomes, L. C., Moreira, J. M. R., Simões, M., Melo, L. F., and Mergulhão, F. J. (2014). Biofilm Localization in the Vertical Wall of Shaking 96-Well Plates. *Scientifica* 2014, 231083. doi:10.1155/2014/231083

Ha, D.-G., and O'Toole, G. A. (2015). c-di-GMP and its Effects on Biofilm Formation and Dispersion: A Pseudomonas Aeruginosa Review. *Microbiol. Spectr.* 3 (2), MB-0003-2014. doi:10.1128/microbiolspec.MB-0003-2014

He, X., Wang, J., Abdoli, L., and Li, H. (2016). Mg2+/Ca2+ Promotes the Adhesion of Marine Bacteria and Algae and Enhances Following Biofilm Formation in Artificial Seawater. *Colloids Surf. B: Biointerfaces* 146, 289–295. doi:10.1016/j.colsurfb.2016.06.029

Herrero, M., and Stuckey, D. C. (2015). Bioaugmentation and its Application in Wastewater Treatment: A Review. *Chemosphere* 140, 119–128. doi:10.1016/j.chemosphere.2014.10.033

Heydorn, A., Nielsen, A. T., Hentzer, M., Sternberg, C., Givskov, M., Ersbøll, B. K., et al. (2000). Quantification of Biofilm Structures by the Novel Computer Program COMSTAT. *Microbiology* 146 (10), 2395–2407. doi:10.1099/00221287-146-10-2395

Hou, X., Liu, S., and Zhang, Z. (2015). Role of Extracellular Polymeric Substance in Determining the High Aggregation Ability of Anammox Sludge. *Water Res.* 75, 51–62. doi:10.1016/j.watres.2015.02.031

Jefferson, K. K. (2004). What Drives Bacteria to Produce a Biofilm? *FEMS Microbiol. Lett.* 236 (2), 163–173. doi:10.1111/j.1574-6968.2004.tb09643.x

Jenal, U., Reinders, A., and Lori, C. (2017). Cyclic Di-GMP: Second Messenger Extraordinaire. *Nat. Rev. Microbiol.* 15 (5), 271–284. doi:10.1038/nrmicro.2016.190

Kaiser, J. P., Feng, Y., and Bollag, J. M. (1996). Microbial Metabolism of Pyridine, Quinoline, Acridine, and Their Derivatives under Aerobic and Anaerobic Conditions. *Microbiol. Rev.* 60 (3), 483–498. doi:10.1128/mr.60.3.483-498.1996

Liang, J., Li, W., Zhang, H., Jiang, X., Wang, L., Liu, X., et al. (2018). Coaggregation Mechanism of Pyridine-Degrading Strains for the Acceleration of the Aerobic Granulation Process. *Chem. Eng. J.* 338, 176–183. doi:10.1016/j.cej.2018.01.029

Liu, Y.-J., and Sun, D. D. (2011). Calcium Augmentation for Enhanced Denitrifying Granulation in Sequencing Batch Reactors. *Process Biochem.* 46 (4), 987–992. doi:10.1016/j.procbio.2011.01.016

Mangwani, N., Shukla, S. K., Rao, T. S., and Das, S. (2014). Calcium-Mediated Modulation of Pseudomonas Mendocina NR802 Biofilm Influences the Phenanthrene Degradation. *Colloids Surf. B: Biointerfaces* 114, 301–309. doi:10.1016/j.colsurfb.2013.10.003

Marciňáková, M., Klingberg, T. D., Lauková, A., and Budde, B. B. (2010). The Effect of pH, Bile and Calcium on the Adhesion Ability of Probiotic Enterococci of Animal Origin to the Porcine Jejunal Epithelial Cell Line IPEC-J2. *Anaerobe* 16 (2), 120–124. doi:10.1016/j.anaerobe.2009.05.001

Mohan, S. V., Sistla, S., Guru, R. K., Prasad, K. K., Kumar, C. S., Ramakrishna, S. V., et al. (2003). Microbial Degradation of Pyridine Using Pseudomonas Sp. And Isolation of Plasmid Responsible for Degradation. *Waste Manage.* 23 (2), 167–171. doi:10.1016/S0956-053x(02)00150-2

O'Toole, G. A., and Kolter, R. (1998). Flagellar and Twitching Motility Are Necessary forPseudomonas Aeruginosabiofilm Development. *Mol. Microbiol.* 30 (2), 295–304. doi:10.1046/j.1365-2958.1998.01062.x

O'Toole, G. A. (2011). Microtiter Dish Biofilm Formation Assay. *J. Vis. Exp.* (47), e2437. doi:10.3791/2437

Parker, J. K., Chen, H., McCarty, S. E., Liu, L. Y., and De La Fuente, L. (2016). Calcium Transcriptionally Regulates the Biofilm Machinery ofXylella Fastidiosato Promote Continued Biofilm Development in Batch Cultures. *Environ. Microbiol.* 18 (5), 1620–1634. doi:10.1111/1462-2920.13242

Passos da Silva, D., Schofield, M., Parsek, M., and Tseng, B. (2017). An Update on the Sociomicrobiology of Quorum Sensing in Gram-Negative Biofilm Development. *Pathogens* 6 (4), 51. doi:10.3390/pathogens6040051

Ramsey, M. M., and Whiteley, M. (2004). *Pseudomonas A* Attachment and Biofilm Development in Dynamic Environments. *Mol. Microbiol.* 53 (4), 1075–1087. doi:10.1111/j.1365-2958.2004.04181.x

Raper, E., Stephenson, T., Anderson, D. R., Fisher, R., and Soares, A. (2018). Industrial Wastewater Treatment through Bioaugmentation. *Process Saf. Environ. Prot.* 118, 178–187. doi:10.1016/j.psep.2018.06.035

Redinbaugh, M. G., and Turley, R. B. (1986). Adaptation of the Bicinchoninic Acid Protein Assay for Use with Microtiter Plates and Sucrose Gradient Fractions. *Anal. Biochem.* 153 (2), 267–271. doi:10.1016/0003-2697(86)90091-6

Renner, L. D., and Weibel, D. B. (2011). Physicochemical Regulation of Biofilm Formation. *MRS Bull.* 36 (5), 347–355. doi:10.1557/mrs.2011.65

Rinaudi, L., Fujishige, N. A., Hirsch, A. M., Banchio, E., Zorreguieta, A., and Giordano, W. (2006). Effects of Nutritional and Environmental Conditions on Sinorhizobium Meliloti Biofilm Formation. *Res. Microbiol.* 157 (9), 867–875. doi:10.1016/j.resmic.2006.06.002

Sezonov, G., Joseleau-Petit, D., and D'Ari, R. (2007). *Escherichia C* Physiology in Luria-Bertani Broth. *J. Bacteriol.* 189 (23), 8746–8749. doi:10.1128/Jb.01368-07

Shen, J., Zhang, X., Chen, D., Liu, X., and Wang, L. (2015). Characteristics of Pyridine Biodegradation by a Novel Bacterial Strain, Rhizobium Sp. NJUST18. *Desalination Water Treat.* 53 (7), 2005–2013. doi:10.1080/19443994.2014.915585

Shukla, S. K., and Rao, T. S. (2013). Effect of Calcium on *Staphylococcus A* Biofilm Architecture: A Confocal Laser Scanning Microscopic Study. *Colloids Surf. B: Biointerfaces* 103 (0), 448–454. doi:10.1016/j.colsurfb.2012.11.003

Simoni, S. F., Bosma, T. N. P., Harms, H., and Zehnder, A. J. B. (2000). Bivalent Cations Increase Both the Subpopulation of Adhering Bacteria and Their Adhesion Efficiency in Sand Columns. *Environ. Sci. Technol.* 34 (6), 1011–1017. doi:10.1021/es990476m

Sims, G. K., Sommers, L. E., and Konopka, A. (1986). Degradation of Pyridine by Micrococcus Luteus Isolated from Soil. *Appl. Environ. Microbiol.* 51 (5), 963–968. doi:10.1128/aem.51.5.963-968.1986

Sobeck, D. C., and Higgins, M. J. (2002). Examination of Three Theories for Mechanisms of Cation-Induced Bioflocculation. *Water Res.* 36 (3), 527–538. doi:10.1016/S0043-1354(01)00254-8

Soni, K. A., Balasubramanian, A. K., Beskok, A., and Pillai, S. D. (2008). Zeta Potential of Selected Bacteria in Drinking Water When Dead, Starved, or Exposed to Minimal and Rich Culture Media. *Curr. Microbiol.* 56 (1), 93–97. doi:10.1007/s00284-007-9046-z

Spangler, C., Böhm, A., Jenal, U., Seifert, R., and Kaever, V. (2010). A Liquid Chromatography-Coupled Tandem Mass Spectrometry Method for Quantitation of Cyclic Di-Guanosine Monophosphate. *J. Microbiol. Methods* 81 (3), 226–231. doi:10.1016/j.mimet.2010.03.020

Stoodley, P., Sauer, K., Davies, D. G., and Costerton, J. W. (2002). Biofilms as Complex Differentiated Communities. *Annu. Rev. Microbiol.* 56, 187–209. doi:10.1146/annurev.micro.56.012302.160705

Thomsen, A. B., and Kilen, H. H. (1998). Wet Oxidation of Quinoline: Intermediates and By-Product Toxicity. *Water Res.* 32 (11), 3353–3361. doi:10.1016/S0043-1354(98)00116-X

Tischler, A. H., Lie, L., Thompson, C. M., and Visick, K. L. (2018). Discovery of Calcium as a Biofilm-Promoting Signal for Vibrio Fischeri Reveals New Phenotypes and Underlying Regulatory Complexity. *J. Bacteriol.* 200 (15), e00016–00018. doi:10.1128/JB.00016-18

Valentini, M., and Filloux, A. (2016). Biofilms and Cyclic Di-GMP (C-Di-GMP) Signaling: Lessons from *Pseudomonas A* and Other Bacteria. *J. Biol. Chem.* 291 (24), 12547–12555. doi:10.1074/jbc.R115.711507

Van Houdt, R., and Michiels, C. W. (2005). Role of Bacterial Cell Surface Structures in *Escherichia C* Biofilm Formation. *Res. Microbiol.* 156 (5-6), 626–633. doi:10.1016/j.resmic.2005.02.005

Vu, B., Chen, M., Crawford, R., and Ivanova, E. (2009). Bacterial Extracellular Polysaccharides Involved in Biofilm Formation. *Molecules* 14 (7), 2535–2554. doi:10.3390/molecules14072535

Wang, T., Flint, S., and Palmer, J. (2019). Magnesium and Calcium Ions: Roles in Bacterial Cell Attachment and Biofilm Structure Maturation. *Biofouling* 35 (9), 959–974. doi:10.1080/08927014.2019.1674811

Wang, Y., Qin, J., Zhou, S., Lin, X., Ye, L., Song, C., et al. (2015). Identification of the Function of Extracellular Polymeric Substances (EPS) in Denitrifying Phosphorus Removal Sludge in the Presence of Copper Ion. *Water Res.* 73, 252–264. doi:10.1016/j.watres.2015.01.034

Wu, Y., Ding, Y., Cohen, Y., and Cao, B. (2015). Elevated Level of the Second Messenger C-Di-GMP in Comamonas Testosteroni Enhances Biofilm Formation and Biofilm-Based Biodegradation of 3-Chloroaniline. *Appl. Microbiol. Biotechnol.* 99 (4), 1967–1976. doi:10.1007/s00253-014-6107-7

Xu, P., Han, H., Zhuang, H., Hou, B., Jia, S., Wang, D., et al. (2015). Anoxic Degradation of Nitrogenous Heterocyclic Compounds by Activated Sludge and Their Active Sites. *J. Environ. Sci.* 31 (5), 221–225. doi:10.1016/j.jes.2014.09.034

Ye, Y., Ling, N., Jiao, R., Wu, Q., Han, Y., and Gao, J. (2015). Effects of Ca2+ and Mg2+ on the Biofilm Formation of Cronobacter Sakazakii Strains from Powdered Infant Formula. *J. Food Saf.* 35 (3), 416–421. doi:10.1111/jfs.12190

Yu, H., Liang, H., Qu, F., He, J., Xu, G., Hu, H., et al. (2016). Biofouling Control by Biostimulation of Quorum-Quenching Bacteria in a Membrane Bioreactor for Wastewater Treatment. *Biotechnol. Bioeng.* 113 (12), 2624–2632. doi:10.1002/bit.26039

Yue, W., Chen, M., Cheng, Z., Xie, L., and Li, M. (2018). Bioaugmentation of Strain Methylobacterium Sp. C1 Towards P-Nitrophenol Removal with Broad Spectrum Coaggregating Bacteria in Sequencing Batch Biofilm Reactors. *J. Hazard. Mater.* 344, 431–440. doi:10.1016/j.jhazmat.2017.10.039

Zhang, Y., Li, C., Wu, Y., Zhang, Y., Zhou, Z., and Cao, B. (2019). A Microfluidic Gradient Mixer-Flow Chamber as a New Tool to Study Biofilm Development under Defined Solute Gradients. *Biotechnol. Bioeng.* 116 (1), 54–64. doi:10.1002/bit.26852

Zhao, B., Ran, X. C., Tian, M., An, Q., and Guo, J. S. (2018a). Assessing the Performance of a Sequencing Batch Biofilm Reactor Bioaugmented with *P. S* Strain XL-2 Treating Ammonium-Rich Wastewater. *Bioresour. Technol.* 270, 70–79. doi:10.1016/j.biortech.2018.09.015

Zhao, Q., Goto, R., Saito, T., Kobayashi, T., and Sasaki, T. (2020). Effect of Gamma-Irradiation on Complexation of Humic Substances with Divalent Calcium Ion. *Chemosphere* 256, 127021. doi:10.1016/j.chemosphere.2020.127021

Zhao, Y., Feng, Y., Li, J., Guo, Y., Chen, L., and Liu, S. (2018b). Insight into the Aggregation Capacity of Anammox Consortia during Reactor Start-Up. *Environ. Sci. Technol.* 52 (6), 3685–3695. doi:10.1021/acs.est.7b06553

Zhou, G., Li, L.-J., Shi, Q.-S., Ouyang, Y.-S., Chen, Y. B., and Hu, W.-F. (2013). Effects of Nutritional and Environmental Conditions on Planktonic Growth and Biofilm Formation of Citrobacter Werkmanii BF-6. *J. Microbiol. Biotechnol.* 23 (12), 1673–1682. doi:10.4014/jmb.1307.0704110.4014/jmb1307.07041

Zhou, G., Shi, Q.-S., Huang, X.-M., and Xie, X.-B. (2016). Proteome Responses of Citrobacter Werkmanii BF-6 Planktonic Cells and Biofilms to Calcium Chloride. *J. Proteomics* 133, 134–143. doi:10.1016/j.jprot.2015.12.019

Conflict of Interest: The authors declare that the research was conducted in the absence of any commercial or financial relationships that could be construed as a potential conflict of interest.

Publisher's Note: All claims expressed in this article are solely those of the authors and do not necessarily represent those of their affiliated organizations, or those of the publisher, the editors and the reviewers. Any product that may be evaluated in this article, or claim that may be made by its manufacturer, is not guaranteed or endorsed by the publisher.